Chemical Engineering Journal 505 (2025) 159607

Contents lists available at ScienceDirect

Chemical Engineering Journal

journal homepage: www.elsevier.com/locate/cej

Sucrose non-fermenting 1-related protein kinase 2–14 participating in lipid elevating efficacy and biodiesel upgrade by *Coccomyxa subllipsoidea*

Yuanyuan Luo [a], Sisi Zhao [a], Zhixuan Fan [a], Yuqin Li [a,*], Zongfan Peng [a], Yulong Zhang [a], Siran Feng [b], Jinhua Mou [c], Zhenyao Wang [b,*], Carol Sze Ki Lin [c], Xuan Li [b]

[a] School of Chemical Engineering, Xiangtan University, Xiangtan 411105, China
[b] Centre for Technology in Water and Wastewater, School of Civil and Environmental Engineering, University of Technology Sydney, Ultimo, NSW 2007, Australia
[c] School of Energy and Environment, City University of Hong Kong, Tat Chee Avenue, Kowloon, Hong Kong, China

ARTICLE INFO

Keywords:
Microalga
SnRK2-14
Gene engineering
Transformants
Fatty acids
Fuel

ABSTRACT

Microalgae-based biodiesel offered a promising solution to mitigate environmental and energy crises, yet improving lipid productivity and upgrading biodiesel quality in microalgae remained a challenge. Abscisic acid (ABA) supplementation to *Coccomyxa subllipsoidea* resulted in lipid accumulation, and most sucrose non-fermenting 1-related protein kinase 2 (*SnRK2*) family genes especially *SnRK2*-14 containing *cis*-acting element for ABA responsiveness in region of promoter showed significant up-regulation and strongly positive correlated with lipid productivity. Therefore, this study was the first to explore the lipid elevating efficacy and biodiesel upgrade by *SnRK2*-14 overexpression in *C. subllipsoidea*. The lipid yield of *SnRK2*-14 overexpression *C. subllipsoidea* strain (*SnRK2*-14-OCS) boosted to 2.18 g/L, representing a 2.63-fold improvement over wild type (WT). Further, *SnRK2*-14 overexpression up-regulated lipid-related genes, rewired intermediates/energy derived from protein and carbohydrate degradation, and inhibited lipid oxidation by strengthening antioxidant capacity to collectively achieve lipid overaccumulation in *SnRK2*-14-OCS. Under fed-batch fermentation mode, the lipid yield further increased 7.92-fold in *SnRK2*-14-OCS compared to WT and also modulated fatty acid profiles to upgrade biodiesel quality to meet the established quality criteria. These findings revealed the involvement of *SnRK2*-14 in lipid biosynthesis in microalgae and highlighted the potential of manipulating *SnRK2*-14 for improved lipid and biodiesel production.

1. Introduction

Conventional fossil fuels reserve depletion triggered a growing concern in exploiting alternative renewable and sustainable energy resources. Biodiesel derived from various biological sources such as animal fat, vegetable oil, or microbial lipids had carved a niche as one of the replacements for fossil fuels [1]. However, using these non-food lipids for biodiesel production were not considered as good alternative to meet the requirement of renewable fuels in food *vs* fuel debate realm [2]. Microalgae were regarded as one of the most valuable candidates for biodiesel production due to rapid growth rates, strong survive ability in adverse conditions, and high lipid accumulation potential to solve energy depletion and alleviate greenhouse effects caused by fossil fuel combustion [3]. Nevertheless, the lipid accumulation efficiency was not well-settled consequently hindered the development of algae-based biodiesel.

Although versatile efforts including strains performances improvement, exogenous chemicals supplementation, culture optimization, and environmental induction were devoted to augment lipid accumulation in microalgae, a gap still existed between the lipid production performance and the lipid yield required for industrial applications [4–6]. Whereas genetic engineering was proposed as feasible strategy to complement current efforts because it could manipulate key genes in carbon metabolic flux pathways to generate more precursors for lipid biosynthesis [7]. For instance, ACS was overexpressed in microalga *Schizochytrium* sp. and *C. reinhardtii* resulting in 1.13-fold increment in fatty acids and 2.4-fold in TAG content [8]; Δ6-FAE overexpression in *N. oceanica* increased the total lipid content by 10.1 % compared to wild type strain [9]; MCAT, PtD5b, and G6PD overexpression in *Phaeodactylum tricornutum* boosted the total lipid content by 55.7 % and polyunsaturated fatty acids to 18.98 μg/mg [10,11]. Other recent studies had met with success by overexpressing endogenous LPAT1 and

* Corresponding authors.
E-mail addresses: yuqinli2004@xtu.edu.cn (Y. Li), Zhenyao.Wang-1@uts.edu.au (Z. Wang).

https://doi.org/10.1016/j.cej.2025.159607
Received 27 November 2024; Received in revised form 7 January 2025; Accepted 13 January 2025
Available online 15 January 2025

DGAT2 in *N. oceanica* to result in 1.6- and 2.1-fold increase of TFAs and TAG, respectively [8]. However, not all of the lipid-related genes were available in enhancing lipid accumulation in microalgae species. The typical exemplification was that a noticeable incensement in lipid content was observed in *P. tricornutum* by overexpressing DGAT whereas no increase in *C. reinhardti* [12,13]. Therefore, using transcription factors to manipulate the abundance of multiple genes relevant to lipid biosynthesis became one of the growing interests. However, transcription factor strategy was still in infancy stage and also identification of TFs regulating lipid pathways of different microalgae species was rather limited [7]. Additionally, the current manipulations of lipid-related genes mainly focused on genes along the lipid pathway, and less attention was paid to upstream genes or key genes in other signaling pathways, which might contribute to industrial production of microalgae-based biodiesel within reach.

Phytohormones signaling pathways offered new opportunities in boosting lipids production, which was crucial in propelling the industrialization of microalgae-biodiesel production [14]. Among these phytohormones, abscisic acid (ABA) had been widely investigated for its promoting effects on the growth and lipid accumulation in multiple algal strains [15–17]. These studies showed that ABA induction could notably upregulate lipid-related genes such as KASI [15], ACAT [18], and DGAT [19], elevate the levels of antioxidant enzymes, and combat reactive oxygen species accumulation, thereby preventing algal lipid peroxidation and facilitating lipid accumulation in microalgae [16,19]. Further analysis of the promoters of some lipid-related genes revealed the presence of multiple ABA-responsive elements in these promoters, confirming that the presence of ABA-responsive elements affected the expression of these lipid-regulatory genes [15]. Moreover, the key components of the ABA signaling pathway directly determined ABA-related activities, which in turn regulated lipid-related gene expression and lipid accumulation in microalgae [15]. Therefore, manipulating these crucial components in ABA signaling pathway could further enhancing lipid accumulation in microalgae. It was well-known that sucrose non-fermenting 1-related protein kinase 2 (*SnRK2*) family genes, as one of the key components in the ABA-receptor coupled core signaling, had been shown to play multiple functions in some plant species [20,21]. For instance, overexpression of *SnRK2* subgroups could assist plants to against drought, salt, and cold stress [22]; *SnRK2* upregulation could also positively promote the biosynthesis of energy compounds such as sugar, lipid, and fatty acids [23]; and *SnRK2* overexpression in *A. cristatum* elevated the levels of superoxide dismutase, peroxidase, and catalase along with the reductions of reactive oxygen species [24]. These clues would be beneficial for oleaginous species since up-regulating *SnRK2* could promote energy compounds biosynthesis and also enhancing antioxidative defense system to protect lipids from oxidative stress consequently boosted the ultimate lipid productivity. Even though the multiple functions of *SnRK2* were explored in some plant species, little information was known about its roles in modulating metabolic activities such as growth and lipid accumulation in microalgae.

Trebouxiophyceaen *Coccomyxa subellipsoidea* as a type of small elongated non-motile unicellular green alga had been gradually served as new oleaginous resources for biodiesel production on account of 1) a relatively-high growth rate and lipid biosynthesis efficacy; 2) the fragile cell wall to simplify lipid extraction and genetic manipulation; 3) psychrotolerant characteristics made mass outdoor cultivation possible by decreasing cost and contamination; and 4) known fully sequenced genome [2]. However, *C. subellipsoidea* was rarely investigated in the aspect of phytohormones culture technologies or strategies even manipulation genes in hormone signaling pathways to target lipid production in *C. sublipsoidea*. Therefore, this study attempted to evaluate the lipid elevating efficacy and biodiesel upgrade by *SnRK2*-14 homologous expression in *C. sublipsoidea*. The outcomes could reveal the involvement of *SnRK2*-14 in lipid biosynthesis in *C. sublipsoidea* and highlight the potential of manipulating *SnRK2*-14 for improved lipid and biodiesel production.

2. Materials and methods

2.1. Microalga strain and culture with abscisic acid

Coccomyxa sublipsoidea C-169 was derived from Collection Center of Algae at National Institute for Environmental Studies (NIES), Japan. The alga was maintained on an Basal medium agar plate that contained consistent compositions with the previous report [2]. A single colony from the agar plate was inoculated into 30 mL of Basal medium under sterile conditions and induced at 28 ℃ with an orbital shaking of 120 rpm and T8 LED fluorescent lamp (three light tubes) as constant light source to provide light irradiance of 50 μmol/m^2/s for 120 h. The lamp specifications were constituted by Light intensity: 1000 ± 50 lx Rated power: 10 W; Wave ranges: 420–740 nm; Life time: 2500–3125 day; Light color temperature: 6000 K; Usage time: 20,000–25,000 h; Reflector specification: 0.02–0.5. *C. sublipsoidea* seed, at a 5 % volume ratio, was inoculated into 100 mL of Basal medium and ABA with filtration sterilization was added separately at initial phase (0 h) and logarithmic phase (96 h) of *C. sublipsoidea* to reach final concentrations of 0, 0.5, 1, 2 and 8 mg/L. *C. sublipsoidea* cells were treated without ABA supplementation as control. All cultures were induced for total 168 h from inoculation to harvest under same culture conditions above.

2.2. Measurement of biomass and lipid

All algal cultures were centrifuged at 8 000 g for 10 min for algal pellets and subsequently lyophilized until constant weight. The biomass was expressed with the weight of lyophilized algal powder divided by culture volume. Up to 20 mg of lyophilized algal powder was mixed with 3.5 mL chloroform/methanol (2:1, v/v) and 1 mL distilled water. All mixed samples were ultra-sonicated for 20 min and centrifugated at 8 000 g for 10 min to collect chloroform layer by three to five cycles. Phases containing lipids were collected by centrifugation at 8 000 g for 10 min and performed vacuum drying until constant weight. Lipid content and lipid yield were calculated as the lipid weight divided by the biomass weight and also the lipid weight divided by culture volume and time.

2.3. Transcriptomic analysis of C. sublipsoidea cells treated with ABA

At the logarithmic growth phase, *C. sublipsoidea* treated with 8 mg/L ABA served as experimental cells, while the untreated cells served as the control for transcriptome analysis. Transcriptomic procedures were performed according to the descriptions of Li et al. (2023) [25] and raw data files were deposited in the National Center for Biotechnology Information (NCBI) Sequence Read Archive (PRJNA1173179). The differentially expression genes (DEGs) between experimental and control cells were identified by using the DESeq2 functions estimateSizeFactors and nbinom Test. $P < 0.05$ was treated as the threshold to indicate significant differential expression. Further, $|\log_2$ Fold Change$| > 1$ and adjusted p-value < 0.05 two standards were employed to indicate the differential expression of the same unigenes between cell samples. The adjusted p-value was the p-value of every unigene adjusted by multiple hypothesis test using the method of false discovery rate. Hierarchical cluster analysis of DEGs was performed to investigate gene expression patterns. GO and KEGG pathway enrichment analyses of DEGs were performed using R based on hypergeometric distribution. The primers of some random DEGs were designed using Primer Premier 6.0 (Table S1). These random DEGs were validated by quantitative real-time polymerase chain reaction (qRT-PCR) and mRNA levels were normalized with 18 s rRNA as the reference by the $2^{-\Delta\Delta Ct}$ method [26]. The reliability of transcriptomic data was built by comparing qRT-PCR expression of random DEGs.

2.4. Bioinformatics analysis of SnRK2 family genes

The correlation relationships between the selected *SnRK2* family genes and lipid-related genes were built by Pearson correlation coefficient to find out the member of *SnRK2* family genes that was the most highly correlated with lipid-related genes. The correlation map was created by using R 4.0.0 and RStudio 4.4.0. The upstream 2 000 bp sequence of the most key member *SnRK2*-14 was extracted from the genome of *C. subllipsoidea* by TBtools and the *cis*-elements were predicted by using the PlantCARE website (http://bioinformatics.psb.ugent.be/webtools /plantcare/html/). The results were visualized by TBtools after redundancy removal. The amino acid sequence of *SnRK2*-14 (Accession number: XM_005650417.1) was retrieved from NCBI (https://www.ncbi.nlm.nih.gov/). The phylogenetic tree was constructed using MEGA11 by neighbor-joining algorithm based on the amino acid sequences of *SnRK2* from some strains such as *C. reinhardtii*, *C. sorokiniana*, *A. thaliana*, and *C. subllipsoidea* to clear the homologies of *SnRK2*-14 gene.

2.5. Cloning, plasmid construction, and C. subllipsoidea transformation of SnRK2-14 gene

Total RNA in logarithmic phase of *C. subllipsoidea* cells was extracted with TRIzol (Sangon, China) and then transcribed into cDNA. The coding sequence of *SnRK2*-14 was amplified by using primers shown in Table S2 and cDNA template. The pCAMBIA1303-*SnRK2*-14 expression vector was constructed by ClonExpress II one step kit (Vazyme, Nanjing, China). Afterward, 4 μg of plasmid DNA, 40 μg of salmon sperm DNA (Invitrogen, California, USA), and 0.2 mL *C. subllipsoidea* cells in logarithmic phase were introduced into an electroporation cuvette (0.2 cm gap, Bio-Rad, USA). The recombinant plasmid was transformed into *C. subllipsoidea* cells under the electroporation parameters (2.7 kV, 25 μF, and 400 Ohm (Ω)). The empty vector pCAMBIA1303 was also introduced into *C. subllipsoidea* cells and used as the control. The electroporated *C. subllipsoidea* cells were transformed into 10 mL Basal medium and induced for 24 h without light exposure. The electroporated cells were spread on a solid Basal medium plate with 20 μg/mL hygromycin to select the positive transformants.

2.6. Molecular verification of SnRK2-14 overexpression C. subllipsoidea strain

SnRK2-14 overexpression *C. subllipsoidea* strain (*SnRK2*-14-OCS) was conducted PCR using universal pCAM primers shown in Table S2. Genomic DNA of both *SnRK2*-14-OCS and WT was isolated using cetyltrimethylammonium bromide method. The integrated pCAMBIA1303-*SnRK2*-14 was amplified using the extracted genomic DNA as the template. The transcript level of *SnRK2*-14 was measured by qRT-PCR according to the descriptions in Section 2.3. Western blotting was performed to detect the expression of pCAMBIA1303 vector own mGFP-tagged protein using an anti-GFP antibody (Invitrogen, California, USA). Actin was used as internal housekeeping control. The enzyme activity of *SnRK2*-14 was also measured using the Plant SnRK protein kinase family member 2 (SnRK2) ELISA kit (Baililai, Shanghai, China) following the manufacturer's instructions.

2.7. Growth and metabolites characterization of SnRK2-14-OCS

Biomass and lipid content of *SnRK2*-14-OCS and WT were measured by the descriptions in Section 2.2. Starch, chlorophyll, carotenoid, and polyphenol metabolites were separately measured with assay kits (Mlbio, Shanghai, China) by the manufacturer's instructions. The crude protein contents were determined by the Kjeldahl nitrogen method including digestion, distillation, and titration [2]. The protein content was expressed as a percentage of mass according to the amount of protein divided by the amount of loaded algal biomass.

2.8. Characterizations of lipid-related genes in SnRK2-14-OCS

The expression levels of acetyl-CoA carboxylase (ACC), fatty acid synthase (FAS), diacylglycerol acyltransferase (DGAT), and fatty acyl-ACP thioesterase A (FATA) were measured by qRT-PCR, and the specific primers are summarized in Table S2. The expressions were normalized with 18S rRNA as reference gene by the $2^{-\Delta\Delta Ct}$ method in Section 2.3. The enzyme activity of ACC, FAS, DGAT, and FATA were measured using assay kits (Mlbio, Shanghai, China) following the manufacturers' instructions.

2.9. Measurement of antioxidant system in SnRK2-14-OCS

The activities of superoxide dismutase (SOD), catalase (CAT), and peroxidase (POD), malondialdehyde (MAD) content, and total antioxidant capacity (T-AOC) were determined by assay kits (Beyotime, China) according to the manufacturers' specifications. Reactive oxygen species (ROS) level was measured by cell-permeable fluorogenic probe 2′,7′-dichlorodihydrofluorescein diacetate (DCFH DA, Beyotime, China).

2.10. Fed-batch fermentation of SnRK2-14-OCS

Seed liquid of *SnRK2*-14-OCS with different volume ratios (2 %, 4 %, 6 %, 8 %, and 10 %) were inoculated into different pH (5.1, 5.6, 6.6, 7.1, and 7.6) and C/N ratio (16, 20, 24, 32, and 48) 100 mL of Basal medium. The pH of Basal medium was adjusted with 0.1 M NaOH or 0.1 M HCl and also C/N ratio was controlled by adding glucose and fixing sodium nitrate. All cultures were induced for 168 h under above culture conditions to determine the optimal growth parameters. The time-course variations of biomass, lipid, carbon and nitrogen consumption were measured under the optimal conditions. These variations were described by kinetic modeling and performed nonlinearly fitting with experimental data [27].

Seed liquid of engineered microalgae with 8 % volume ratio (OD_{680} = 0.1) was inoculated into 1 L of Basal medium (pH = 5.6) to conduct fed-batch fermentation cultivation under above temperature, light availability, and orbital shaking. Glucose and sodium nitrate at fermentation beginning were 20 g/L and 1.5 g/L (i.e., C/N = 32). The reducing sugar concentration (RSC) was controlled at 5 ~ 20 g/L by supplementation glucose at designated 48, 60, and 72 h intervals. The variations in biomass, lipid, RSC, and total nitrogen (TN) were measured at 12–24 h intervals. RSC and TN were detected by 3, 5-dinitrosalicylic acid and alkaline potassium persulfate digestion UV-spectrophotometer [28].

2.11. Evaluation of biodiesel properties by SnRK2-14-OCS

The resulting fatty acid methyl esters (FAMEs) were prepared by the descriptions in the report of Li et al. [25]. FAMEs were analyzed using an Agilent 7890A capillary gas chromatograph equipped with a 5975C mass spectrometry detector and an HP-88 capillary column (60 m × 0.25 mm; Agilent Technologies, Wilmington, DE, USA). C17:0 was supplemented into samples as the internal standard prior to transesterification. The individual FAMEs were identified and quantified by comparison with authentic standards (Sigma-Aldrich, MO, USA). The properties of *SnRK2*-14-OCS-based biodiesel were evaluated by encompassing theoretical calculations of various chemical and physical indicators, including average degree of unsaturation (ADU), cetane number (CN), iodine value (IV), kinematic viscosity (νi), specific gravity (ρ), cloud point (C), long chain saturation factor (LCSF), higher heating value (HHV), and cold filter plugging point (CFPP) [2].

2.12. Statistical analysis

All experiments were performed with biological triplicates and data were expressed as means ± standard deviation (SD). Statistical analysis

was carried out using IBM SPSS Statistics 26.0 (Armonk, USA). Differences in groups were analyzed for significance using one-way analysis of variance (ANOVA) and compared using student's *t*-test [$p < 0.05$ (*), $p < 0.01$ (**), and $p < 0.001$ (***)].

3. Results and discussion

3.1. ABA induction affected the growth and lipid content in *C. sublipsoidea*

It was well-documented that ABA exhibited diverse effects on the growth of microalgae in light of species-specific and supplementation at different growth phase [15,29,30]. As observed in Fig. 1a that ABA supplementation at the initial culture phase depressed the growth of *C. sublipsoidea*. Specifically, when ABA were increased from 0.5 ~ 8 mg/L, the biomass was separately achieved by 3.16, 3.11, 3.10, 3.09, and 2.92 g/L, which presented 1.02- to 1.08-fold reductions in comparison with the control (0 mg/L). This was consistent with the previous report where the biomass of *C. vulgaris* treated with ABA presented significant decrease in comparison without ABA treatment [15]. When ABA supplementation at logarithmic phase of *C. sublipsoidea* caused increase in biomass (Fig. 1b). The maximum biomass of 3.22 g/L was achieved by 1.0 mg/L ABA, increasing by 1.02- and 1.04-fold more than that of supplementation at initial phase and control. Similar phenomena was also observed in *Chlorella* sp. and *C. zofingiensis* that the biomasses were boosted under ABA treatment [17,31]. The previous reports once suggested that phytohormones were one of the vital factors to affect biomass accumulation in microalgae by means of mediating cell growth cycle (growth phase 1-G1, DNA synthetic phase-S, growth phase 2-G2, and mitosis-M) and transition points (G1/S and G2/M) [32,33]. However, each type of phytohormone manipulated the cell growth cycle differently. Liu et al. (2017) found that ABA specifically inhibited the DNA replication and block G1/S transition of cell growth cycle in some alga species consequently resulted in the reduced biomass [34]. Therefore, the potential possibilities of above phenomenon could be that ABA supplementation at the logarithmic phase bypassed the critical period where ABA addition at lag growth phase hindered DNA replication and block G1/S transition of cell growth cycle to benefit biomass accumulation to a certain degree [34]. These findings demonstrated that ABA supplementation affected the growth behavior, especially supplementation at logarithmic phase was more favorable to promote the growth of *C. sublipsoidea*.

Although ABA supplementation at initial culture phase was less impressive in promoting cell growth of *C. sublipsoidea*, it showed a positive action in elevating lipid accumulation with dose-dependent effects (Fig. 1c). Specifically, the lipid content increased from 33.75 % to 36.75 % with ABA increment from 0.5 to 8 mg/L and the highest lipid content with 8 mg/L ABA supplementation represented 1.40-fold more than that of the control. This agreed with the reports that ABA treatment exhibited more effective lipid accumulation in *P. tricornutum* [19]. However, an intriguing case was that ABA supplementation (0.5 ~ 8 mg/L) at the logarithmic phase of *C. sublipsoidea* led to a more notable increase in lipid content than at initial culture phase and control (Fig. 1d). The highest lipid content of 45.50 % was achieved at 8 mg/L ABA, representing an obvious up-regulation over ABA supplementation at initial culture stage and the control. This suggested that ABA supplementation at the logarithmic phase was more beneficial for lipid accumulation in *C. sublipsoidea*. Additionally, this boosting effect was also reflected in the lipid yield that 8 mg/L ABA supplementation at the logarithmic phase achieved the highest lipid yield by 1.45 g/L, representing 1.33– to 1.69-fold more than that of initial phase supplementation and control (Fig. 1e–f). Therefore, combining biomass, lipid content, and lipid yield, 8 mg/L ABA addition at the logarithmic phase was the most beneficial strategy for *C. sublipsoidea*.

3.2. SnRK2-14 and lipid-related genes up-regulated in transcriptome of *C. sublipsoidea* treated with ABA

Totally 534 up-regulated genes and 568 down-regulated genes were recognized as DEGs by comparing the transcriptomic profiles of *C. sublipsoidea* cells treated with ABA and without ABA (Fig. 2a). The expression levels of four randomly selected DEGs performed a positive correlation between mRNA-Seq and qRT-PCR and verified the reliability of transcriptome data (Fig. 2b). After filtering out putative or unknown genes and following certain screening rules, 512 DEGs were annotated using GO and KEGG databases to identify the functional and biological pathways. Go enrichment analysis revealed that DEGs mainly 1) participated in phosphorylation, transmembrane transport, and methylation biological process; 2) involved in the cellular component of cytoplasm; and 3) possessed ATP binding, hydrolase, and oxidoreductase activity (Fig. 2c). KEGG enrichment analysis indicated that DEGs were associated with carbohydrate metabolism, lipid biosynthesis, and signal transduction (Fig. 2d). Since this study focused on the effects of ABA treatment on lipid accumulation, twenty-eight DEGs responded to ABA signal transduction pathway and lipid biosynthesis were further discussed in detail (Fig. 2e).

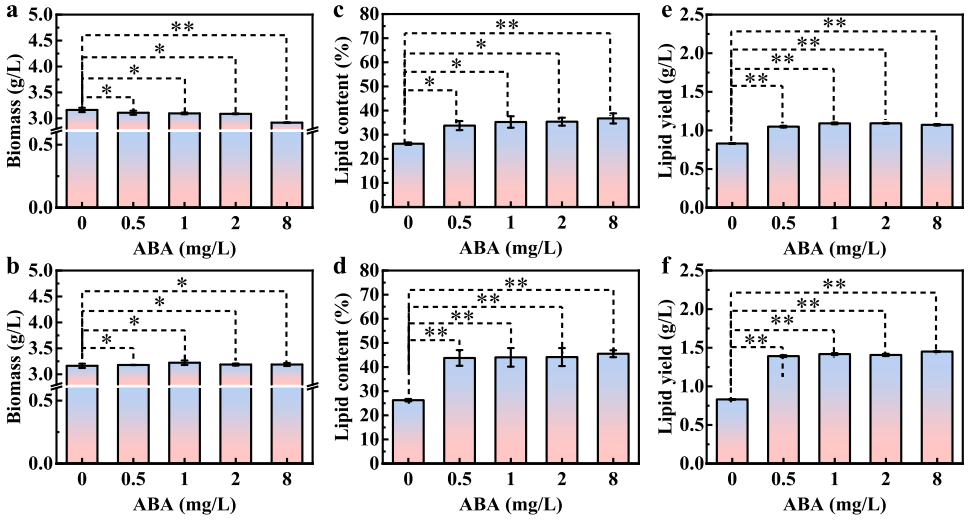

Fig. 1. The effects of different ABA supplementation at the initial growth phase (a, c, and e) and logarithmic growth phase (b, d, and f) of *C. sublipsoidea* on the biomass, lipid content, and lipid yield. ABA represented abscisic acid. Data were presented as means of three biological replicates ± SD.

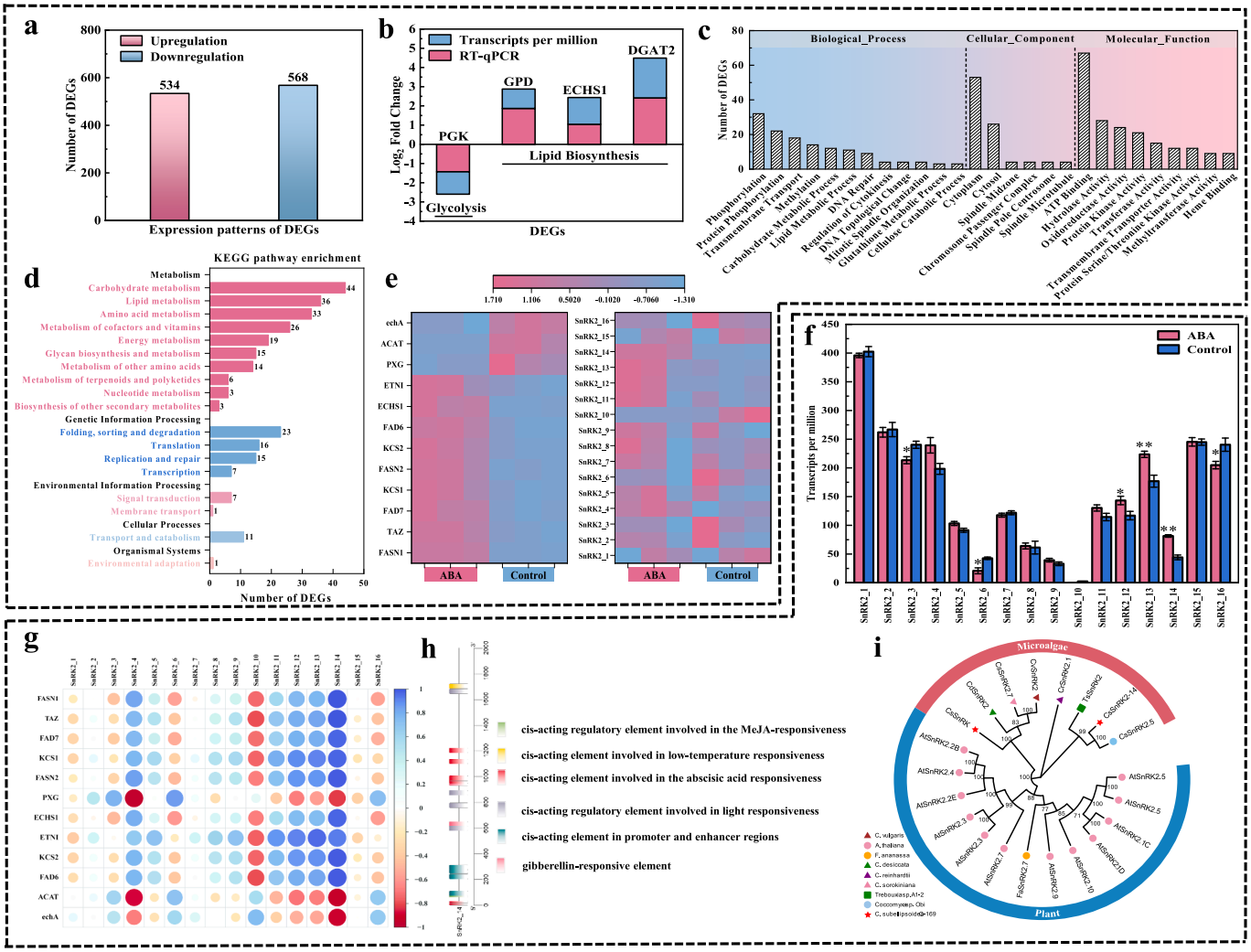

Fig. 2. Effects of ABA supplementation on lipid-related genes and *SnRK2* family genes in *C. subllipsoidea* cells. Number and expression patterns of DEGs in *C. subllipsoidea* cells treated with ABA (a); RNASeq expression pattern and qRT-PCR expression pattern comparison of the representative DEGs (b); Gene Ontology (GO) classification and Kyoto Encyclopedia of Genes and Genomes (KEGG) pathway annotation of DEGs (c-d); The heat-map analysis of 12 lipid-related genes and 16 *SnRK2* family genes in ABA signal transduction pathway (e); The transcripts per million of 16 *SnRK2* family genes in ABA signal pathway (f); The correlation circle map of 12 lipid-related genes and 16 *SnRK2* family genes in ABA signal pathway (g), the colors (blue and red separately indicating positive and negative correlations) represented the correlation coefficient between lipid-related genes and *SnRK2* family genes; The *cis*-acting motif prediction of *SnRK2*-14 gene in ABA signal pathway (h); Phylogenetic tree analysis between *SnRK2*-14 amino acid sequence in *C. subllipsoidea* and the identified *SnRK2* sequences in other species (i). DEGs represented the differentially expressed genes. PGK, GPD, ECHS1, DGAT2, echA, ACAT, PXG, ETNI, ECHS1, FAD6, FASN2, KCS1, KCS2, FAD7, TAZ, FASN1, and SnRK2 represented phosphoglycerate kinase, glyceraldehyde-3-phosphate dehydrogenase, enoyl CoA hydratase 1, diacylglyceryl acyltransferase 2, enoyl-CoA hydratase, acetyl-CoA acetyltransferase, peroxygenase, ethanolamine-phosphate phospho-lyase, enoyl-CoA hydratase, fatty acid desaturase 6, fatty acid synthase 2, ketoacyl CoA synthase 1 and 2, fatty acid desaturase 7, monolysocardiolipin acyltransferase, fatty acid synthase, and sucrose non-fermenting 1-related protein kinase 2. (For interpretation of the references to color in this figure legend, the reader is referred to the web version of this article.)

Twelve DEGs, namely enoyl-CoA hydratase (echA), acetyl-CoA acetyltransferase (ACAT), peroxygenase (PXG), ethanolamine-phosphate lyase (ETNI), enoyl-CoA hydratase (ECHS1), fatty acid desaturase 6 (FAD6), ketoacyl-CoA synthase 2 (KCS2), fatty acid synthase 2 (FASN2), ketoacyl CoA synthase 1 (KCS1), fatty acid desaturase 7 (FAD7), monolysocardiolipin acyltransferase (TAZ), and fatty acid synthase 1 (FASN1), were identified as lipid-related genes of interest (Fig. 2e). Among these genes, TAZ, ECHS1, ETN1, FAD7, FAD6, KCS1, KCS2, FASN1, and FASN2 were reported to catalyze the elongation of C16 and C18-CoA of the acyl-CoA pool and also desaturation reactions to form double bond at specific positions in the acyl chain [35,36]. And the nine genes presented 2.08- to 24.40-fold up-regulations in *C. subllipsoidea* cells treated with ABA compared to control (Fig. 2e). This showed consistence with some investigations where the genes responsible for fatty acid biosynthesis were significantly up-regulated in *P. tricornutum*, *C. pyrenoidosa* FACHB-5, *C. vulgaris* UMT-M1, *C. pyrenoidosa*, and *Chlorella* sp. FACHB-8 under ABA induction [15–17,19,29]. Further, some recent reports found that the up-regulations of KCS1 and KCS2 showed a positive correlation with the long chain fatty acids content in *Schizochytrium* sp. mutants and also the enhancement of FAD6 and FAD7 at the transcript levels supported the significant α-linolenic acid accumulation in *A. protothecoides* [35,36]. Therefore, ABA could induce the up-regulations of these lipid-related genes in this study to contribute lipid biosynthesis in *C. subllipsoidea*. However, a recent report mentioned that the promoter region of lipid-related genes contained multiple ABA-responsive elements and ABA utilized these response elements to regulate gene expression to promote lipid accumulation [15]. Possibly, these lipid-related genes in this study used ABA-responsive elements to build relations with ABA induction consequently promoted lipid biosynthesis, but which key components in ABA signaling

pathway playing a role needed further investigation in depth. Another three genes (i.e., PXG, echA, and ACAT) responsible for lipid oxidation showed 2.10- to 13.04-fold down-regulations response to ABA induction, which indicated the inhibited lipid peroxidation. This was also an important strategy to increase lipid content by suppressing genes responsible for lipid oxidation [37]. Such strategy received supports from some exemplifications where the down-regulation or knockdown of lipid β-oxidation genes were positively correlated to lipid content in *A. protothecoides*, *Chlorella* sp. T4, and *P. tricornutu* [35,37,38]. However, it was worth mentioned that a notable upregulation of ACAT with fatty acid accumulation trend was observed in mutated algal species of *Isochrysis* sp., which diametrically opposed outputs to this study [18]. This discrepancy might be due to that the alga strains used in the two groups of studies were different, on the other hand, the mutation of wild *Isochrysis* led to the up-regulation of ACAT gene and recombined the metabolic pathway to promote lipid synthesis. Collectively, these variations in gene expression contributed the lipid accumulation in *C. subllipsoidea* treated with ABA.

Another interesting phenomenon was that sixteen sucrose non-fermenting 1-related protein kinase 2 (*SnRK2*) family genes were detected in *C. subllipsoidea* treated with ABA and most of them showed significant up-regulations (Fig. 2e–f). For instance, the transcript levels of *SnRK2*-4–5, *SnRK2*-8–9, *SnRK2*-11–16 separately up-regulated 1.05- to 1.84-fold more than that of control. Actually, multiple *SnRK2* family genes were also detected in many species (e.g., *Arabidopsis*, *S. tamariscina*, and *P. patens*) under ABA activation and confirmed the main effects in promoting growth development and controlling abiotic stress responses in plant [39]. Early, *SnRK2*s from the semiterrestrial alga *Klebsormidium nitens* and microalga *C. reinhardtii* were also found to include all ABA signaling elements [39,40]. The concrete situations were that *SnRK2* upregulation could assist microalgae to accumulate energy metabolites (i.e., carbohydrates, lipid, and protein) to against nutrient limitation stress such as nitrogen or phosphorus depletion [40,41]. Of the multiple *SnRK2* genotypes detected in this study, *SnRK2*-4 and *SnRK2*-14 presented the most significant up-regulations by 1.21- and 1.84- fold in *C. subllipsoidea* treated with ABA compared to control.

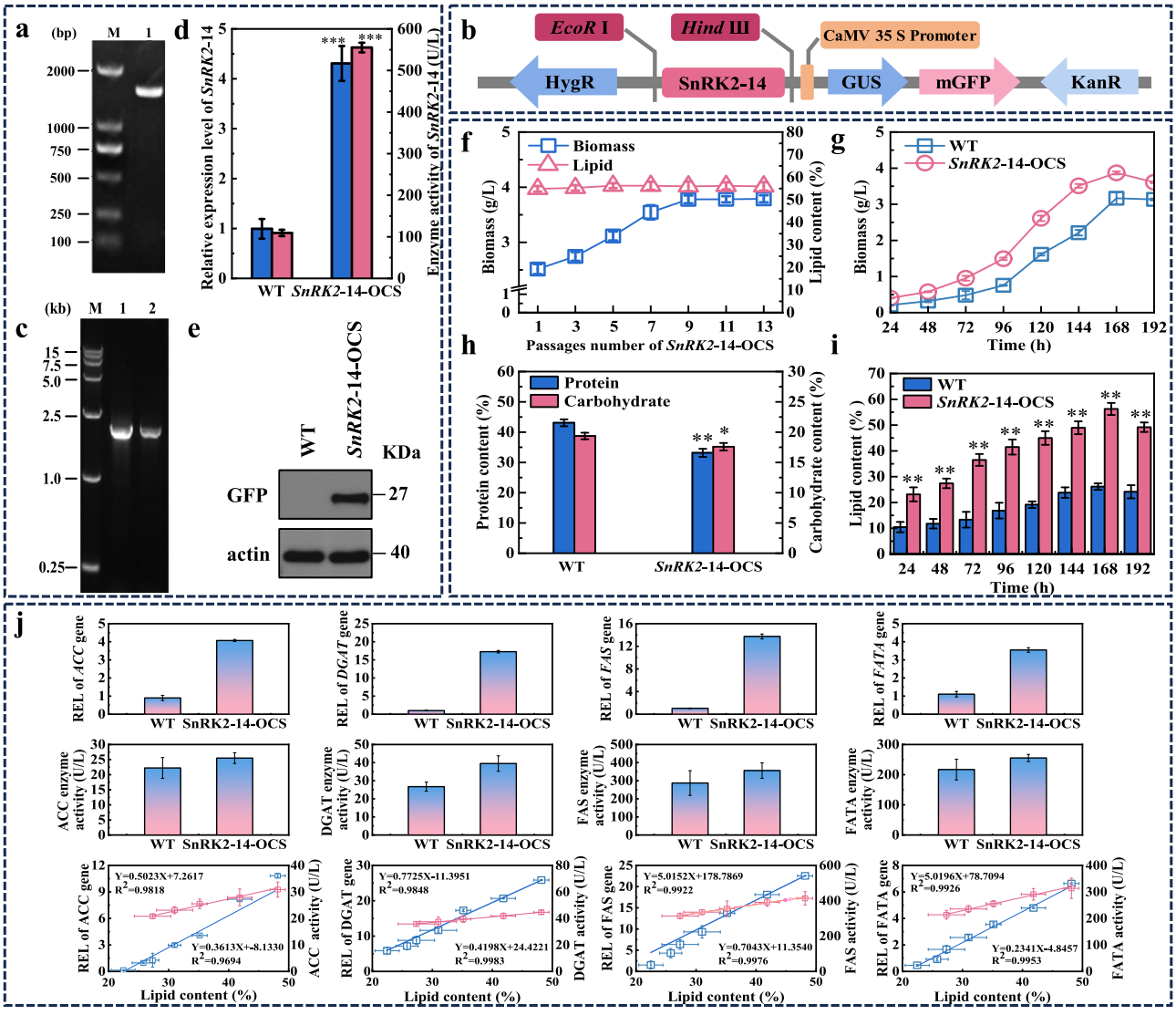

Fig. 3. Cloning and transformation of *SnRK2*-14 gene *into C. subllipsoidea* and biochemical characteristics of *SnRK2*-14-OCS. PCR amplification band of *SnRK2*-14 gene (a); Construction diagram of expression vector pCAMBIA1303-*SnRK2*-14 for *SnRK2*-14 gene (b); PCR amplification band of pCAMBIA1303-*SnRK2*-14 expression vector (c); Relative expression level and enzyme activity of *SnRK2*-14 in *SnRK2*-14-OCS and WT (d). Western blot band graph of *SnRK2*-14 gene expression protein (e); Effects of *SnRK2*-14 overexpression on cell passage, biomass, lipid content, and cellular primary metabolites in *SnRK2*-14-OCS (f-i); Effects of *SnRK2*-14 overexpression on genes and enzymes involved in lipid biosynthesis and also the linear correlations between relative expression level (REL) of lipid-related genes, enzyme activity, and lipid content in *SnRK2*-14-OCS (j). *ACC*, *DGAT*, *FAS*, and *FATA* represented acetyl-CoA carboxylase, diacylglycerol acyltransferase, fatty acid synthase, and fatty acyl-ACP thioesterase and also the genes encoding enzymes. Data were presented as means of three biological replicates ± SD.

Further, correlation analysis between the 12 lipid-related genes and 16 *SnRK2* family genes showed that *SnRK2*-4 and *SnRK2*-14 exhibited strong positive correlation with lipid-related genes and negative correlation with genes involved in fatty acid oxidation and degradation (Fig. 2g). Whereas *SnRK2*-14 showed the strongest positive and negative correlations to 12 lipid-related genes ($p < 0.05$) (Fig. 2g). This demonstrated that *SnRK2*-14 made a most intense response to ABA treatment in oleaginous *C. subllipsoidea*. Further *cis*-acting elements analysis revealed the presence of multiple ABA-responsive elements in the promoter region of *SnRK2*-14 in addition to low temperature, light, and other phytohormone-responsive elements (Fig. 2h). And a phylogenetic analysis clearly exhibited that *SnRK2*-14 protein was highly homologous with *SnRK2* (*Coccomyxa* sp. obi) and *SnRK2* (*Trebouxia* sp. A1-2) (Fig. 2i), which were reported to be more relevant in promoting lipid synthesis [42,43]. Therefore, based on above clues and background, *SnRK2*-14 gene in ABA signal transduction pathway might possess potential function in elevating lipid accumulation in *C. subllipsoidea*. The following section would reveal lipid accumulation function of *SnRK2*-14 by gene homologous expression strategy.

3.3. SnRK2-14 overexpression altered biochemical indices of SnRK2-14-OCS

It could be observed in Fig. 3a that *SnRK2*-14 gene was amplified by PCR to result in 1.8 Kb band in size, which was consistent with the reported band size from NCBI. Subsequently, *SnRK2*-14 PCR product was used to construct the expression vector pCAMBIA1303-*SnRK2*-14 with mGFP tag by the strategy shown in Fig. 3b and electroporated into *C. subllipsoidea* to perform *SnRK2*-14 gene continuous overexpression. The expression vector pCAMBIA1303 with *SnRK2*-14 gene was further amplified by PCR to result in specific band composed of target *SnRK2*-14 gene and part sequence of vector, indicating that *SnRK2*-14 was successfully integrated into the genome of *C. subllipsoidea* (Fig. 3c). Relative expression level and enzyme activity of *SnRK2*-14 in *SnRK2*-14-OCS presented 4.34- and 5.08-fold up-regulations in comparison with wild type (WT) (Fig. 3d). And western blot result showed that the actin protein as housekeeping protein presented in *SnRK2*-14-OCS and WT whereas a specific band of mGFP protein was only present in *SnRK2*-14-OCS (Fig. 3e). These results confirmed that *SnRK2*-14 gene not only was integrated into the genome of *C. subllipsoidea* but also achieved stable expression in transformants.

Overexpression of transgenes usually affected the cellular physiological status, but overexpression without a compromised biomass had been considered a general requirement in subsequent industrial applications [10]. The passage results of this study showed that *SnRK2*-14-OCS experiencing 1–13 passages still had the relatively-stable biomass and lipid content, which indicated hereditary stability and would be superior strain characteristics (Fig. 3f). Additionally, the growth of *SnRK2*-14-OCS and WT showed consistent variation trend by initial increase and then reduction, but the biomass levels of *SnRK2*-14-OCS were higher than that of the WT during the whole culture process (Fig. 3g). Especially, the biomass of *SnRK2*-14-OCS achieved maximal value of 3.87 g/L at 168 h, representing 1.22-fold more than that of the WT. This indicated that the cell growth of *SnRK2*-14-OCS was not affected and *SnRK2*-14 overexpression positively correlated with the growth, which agreed with the investigations where *SnRK2* gene overexpression elevated the growth of *Malus domestica* and *V. corymbosum* [44,45]. Synchronously, it could also be found in Fig. 3h that *SnRK2*-14 overexpression affected intracellular metabolites. The contents in carbohydrate and protein decreased from 19.37 % and 43.09 % to 17.59 % and 33.17 %, respectively, representing 1.10-fold and 1.30-fold reductions in comparison with WT. A previous report noted that a decrease in carbohydrate and protein could contribute more acetyl-CoA precursor and energy into lipid biosynthesis pathway to promote lipid accumulation [46]. Whereas the results in Fig. 3i accorded with this conclusion that the lipid content of *SnRK2*-14-OCS reached 56.27 % at 168 h, representing 2.15-fold higher than of WT. This indicated that the admirable lipid biosynthesis in *SnRK2*-14-OCS might be because *SnRK2*-14 overexpression drove carbon flux/energy generated from carbohydrate and protein degradation into lipid accumulation. Not just these affected metabolites, *SnRK2*-14 overexpression also up-regulated some lipid-related genes in *SnRK2*-14-OCS (Fig. 3j). Specifically, the expression levels of ACC, DGAT, FAS, and FATA in *SnRK2*-14-OCS separately showed 4.53-, 17.32–, 13.21-, 3.20-fold more than that of the WT. Correspondingly, the activity of enzymes encoded by these genes also showed consistent up-regulations in *SnRK2*-14-OCS. The activity of ACC, DGAT, FAS, and FATA were 25.5, 39.49, 355.8, and 255.40 U/L, respectively, which were 1.15- to 1.48-fold higher than that of the WT. Further, the correlation coefficient (R^2) values between the gene expressed levels of ACC, DGAT, FAS, and FATA triggered by *SnRK2*-14 overexpression and lipid content were separately 0.969, 0.985, 0.998, and 0.995, indicating strong linear relationships in *SnRK2*-14-OCS (Fig. 3j). Additionally, the correlation coefficient (R^2) values between enzyme activities (ACC, DGAT, FAS, and FATA) and lipid content were 0.982, 0.998, 0.992, and 0.993, also indicating significant correlations (Fig. 3j). These demonstrated that *SnRK2*-14 overexpression activated these lipid-related genes to regulate lipid accumulation in *SnRK2*-14-OCS.

SnRK2-14 overexpression also significantly increased the activities of SOD, CAT, and POD and the activity was 60.02, 134.69, and 11,424 U/g in *SnRK2*-14-OCS, representing 1.72-, 2.54-, and 2,06-fold more than that of WT ($p < 0.01$) (Fig. 4a). The previous investigation indicated that the up-regulations of anti-oxidases resulted in the enhancement of the total antioxidant capacity (T-AOC) and the reduction of reactive oxygen species (ROS) in *Monoraphidium* [47]. Whereas the results in Fig. 4b met with such results that the intracellular ROS level was reduced by 1.53-fold and T-AOC was enhanced by 2.52-fold in *SnRK2*-14-OCS than in WT. This showed also consistence with the findings that *SnRK2* overexpression in yeast and tobacco elevated the levels of SOD, POD, and CAT and reduced ROS accumulation [48]. Additionally, many findings also indicated that the up-regulations of anti-oxidases and ROS accumulation reduction could alleviate oxidative stress and hindered the oxidative attack of oxygen on lipids consequently increased the lipid content [49]. The expression results of anti-oxidases and ROS shown in Fig. 3 were also highly correlated with the lipid content in *SnRK2*-14-OCS. Therefore, except for *SnRK2-14* overexpression regulating lipid-related genes and driving intermediate metabolites and energy into lipid pathway to promote lipid accumulation, another potential case in increasing lipid accumulation in *SnRK2*-14-OCS was that *SnRK2*-14 overexpression up-regulated anti-oxidases and T-AOC to effectively inhibit the lipid oxidative damage. The results shown in Fig. 4b that MAD content was reduced from 4.83 nM/g to 2.36 nM/g in *SnRK2*-14-OCS also supported this finding. Actually, the most guaranteed way to remove ROS in microalgae cells to protect lipids from oxidative attack was to enhance antioxidant enzymes and also synthesize antioxidant compounds [50,51]. Whereas the results shown in Fig. 4c that the contents of chlorophyll, carotenoids, and polyphenols in *SnRK2*-14-OCS presented 1.49-, 1.53-, and 1.67-fold more than that of WT. Carotenoids combined with chlorophyll daylighting complex LHC and transferred energy to chlorophyll by absorbing blue-green light to promote photosynthesis, and could also directly obtain energy from singlet oxygen to inhibit ROS generation [52]. Further, Telussa et al. (2019) indicated that the increased Car/Chl ratio in microalgae belonged to oxidative stress response, which could effectively prevent cells photo-oxidative damage [53]. Whereas the intracellular carotenoid content and the Car/Chl ratio increased from 11.28 mg/kg to 17.22 mg/kg and 1.32 to 1.36, respectively, suggesting that *SnRK2*-14 overexpression might reduce the photo-oxidative damage of *SnRK2*-14-OCS and provide antioxidant protection barrier for lipid accumulation. Additionally, polyphenols compounds could exert antioxidant effects by single-electron transfer and hydrogen atom transfer reaction capabilities, and had been proven to have significant functions in enhancing the antioxidant ability of algal

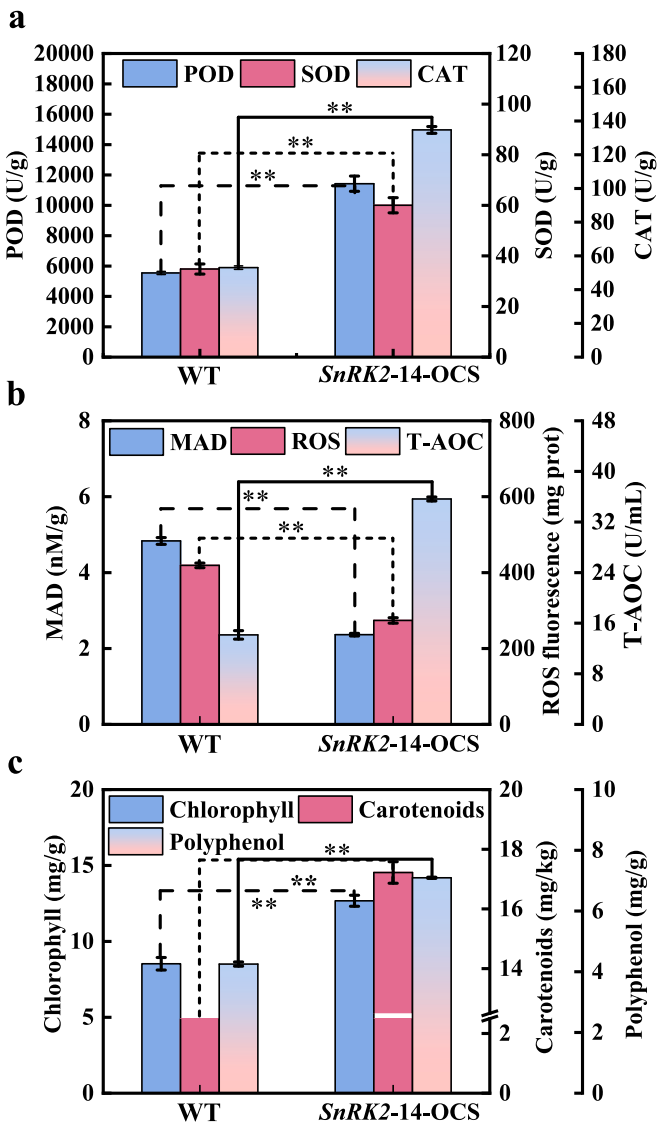

Fig. 4. Effects of *SnRK2*-14 overexpression on antioxidant system of *SnRK2*-14-OCS. Variations in anti-oxidases activity of *SnRK2*-14-OCS and WT (a); Variations in total antioxidant capacity of *SnRK2*-14-OCS and WT (b); Variations in antioxidant compounds of *SnRK2*-14-OCS (c). POD, SOD, CAT, MAD, ROS, and T-AOC represented peroxidase, superoxide dismutase, catalase, malondialdehyde, reactive oxygen species, and total antioxidant capacity, respectively. Data were presented as means of three biological replicates ± SD.

cells [54]. It could be observed from Fig. 4c that the polyphenols content reached 7.25 mg/g in *SnRK2*-14-OCS, representing 1.60-fold more than that of WT. Therefore, *SnRK2*-14 overexpression also strengthened polyphenols antioxidant signaling pathway to inhibit oxidation attack on lipid and achieve lipid accumulation in *SnRK2*-14-OCS.

3.4. SnRK2-14-OCS exhibited robust lipid production under fed-batch fermentation

The aforementioned results demonstrated that *SnRK2*-14 overexpression caused the variations in biochemical properties of *SnRK2*-14-OCS. Re-optimizing the fermentative conditions was the precondition in boosting the growth and lipid yield of *SnRK2*-14-OCS for further industrial biodiesel. As illustrated in Fig. 5a, the biomass and lipid yield exhibited an initial increase and then a decrease in the pH range of 5.1–7.1. The highest biomass and lipid yield of 3.96 g/L and 2.25 g/L, respectively, were achieved at pH 5.6 for *SnRK2*-14-OCS, reflecting a 1.25- and 2.71-fold increase compared to WT, whose optimal pH was 6.1. The discrepancy might be due to that *SnRK2*-14 overexpression regulated *SnRK2*-14-OCS to be more adaptable to relatively acidic environments. The previous reports indicated that non-acidophilic microalgae could exhibit lipid accumulation phenotype to withstand acidic environments stress [55]. Therefore, the high lipid accumulation behavior of *SnRK2*-14-OCS was a stress response to acidic environment. The biomass and lipid yield of *SnRK2*-14-OCS also exhibited initial increase followed by slight decline as the inoculation ratio raised from 2 % to 10 % under optimal pH 5.6 (Fig. 5b). Notably, the biomass and lipid yield peaked 3.93 g/L and 2.29 g/L at an inoculation ratio of 8 %, which were basically-equivalent with the optimal pH but represented 1.24- and 2.76-fold more than that of WT. Further, the biomass and lipid yield of *SnRK2*-14-OCS performed continuous increases with C/N ratio from 20 to 32 and reached the maximum values by 5.05 g/L and 3.09 g/L, exceeding the lower C/N ratio 16 and WT (Fig. 5c). When C/N ratio was boosted to 48, the biomass and lipid yield were depressed. Actually, the carbon in lower C/N ratio was insufficient for metabolic activities of microalgae consequently resulted in decreased activity and worse biomass and lipid production. Whereas the carbon in higher C/N ratio also accompanied with the drops of biomass and lipid since the high carbon substrate inhibition [56]. These indicated that the optimal way to boost growth and lipid production of *SnRK2*-14-OCS was a fermentation condition with pH 5.6, inoculation ratio of 8 %, and C/N ratio of 32.

The variations of reducing sugar concentration (RSC), total nitrogen (TN), biomass, and lipid throughout the whole batch cultivation under the optimal conditions above were delineated in Fig. 5d. The growth and lipid yield of *SnRK2*-14-OCS displayed characteristic *S*-shaped curves. Subsequently, the logistic model equation successfully described and the varying values of biomass and lipid yield. And the nonlinearly fitted results demonstrated the strong agreement between the calculated logistic equation mode values and experimental data, with R^2 of 0.988 and 0.999 for biomass and lipid yield. Additionally, as observed in Fig. 5d, Logistic incorporated Luedeking-Piret model well represented the consumption kinetic of TN and RSC. The experimental data and the simulated values corresponded to together correctly with R^2 of 0.999 and 0.996 for TN and RSC. These fitting results accurately reflected the dynamic changes in RSC, TN, biomass, and lipid yield of *SnRK2*-14-OCS under the optimal conditions above. Additionally, the fermentation kinetics model in Fig. 5d hinted that lipid accumulation operated as a growth-coupled process and biomass was directly proportional to lipid yield. Another crucial information was that the biomass and lipid yield showed significant increments as well as TN and RSC were consumed dramatically between 48 and 96 h. This would offer practical guidance for further elevating the growth and lipid in *SnRK2*-14-OCS by fed-batch fermentation with substrates supplementation at these time points.

The time-course of biomass, lipid yield, RSC, and TN of *SnRK2*-14-OCS by supplementing glucose at designated 48 h, 72 h, and 96 h intervals were presented in Fig. 5e–g. When *SnRK2*-14-OCS experienced fed-batch fermentation with quartic glucose supplementation total 64.27 g/L at 48 h interval, the biomass production and the total lipid yield were gradually increased from 0.1 to 8.99 g/L and 0.20 g/L to 5.94 g/L, representing 1.78- and 1.92-fold more than that of batch mode above. Additionally, RSC exhibited a decreasing trend with each feeding cycle, indicating that *SnRK2*-14-OCS could efficiently consume the available reducing sugar in culture system. The residual RSC was 8.79 g/L at fed-batch fermentation terminal and RSC utilization rate reached 89.56 % by 48 h interval feeding (Fig. 5e). This demonstrated that glucose feeding with 48 h interval was somewhat frequent and *SnRK2*-14-OCS were unable to fully utilize RSC of culture system. Synchronously, TN consumption was also gradually decreased along with the time-course of biomass and lipid yield and the final utilization rate was 91.69 %. Interestingly, *SnRK2*-14-OCS achieved the highest biomass (9.22 g/L) and total lipid yield (6.57 g/L) by three glucose supplementations total 52.80 g/L at 60 h interval, which showed 1.03-fold and

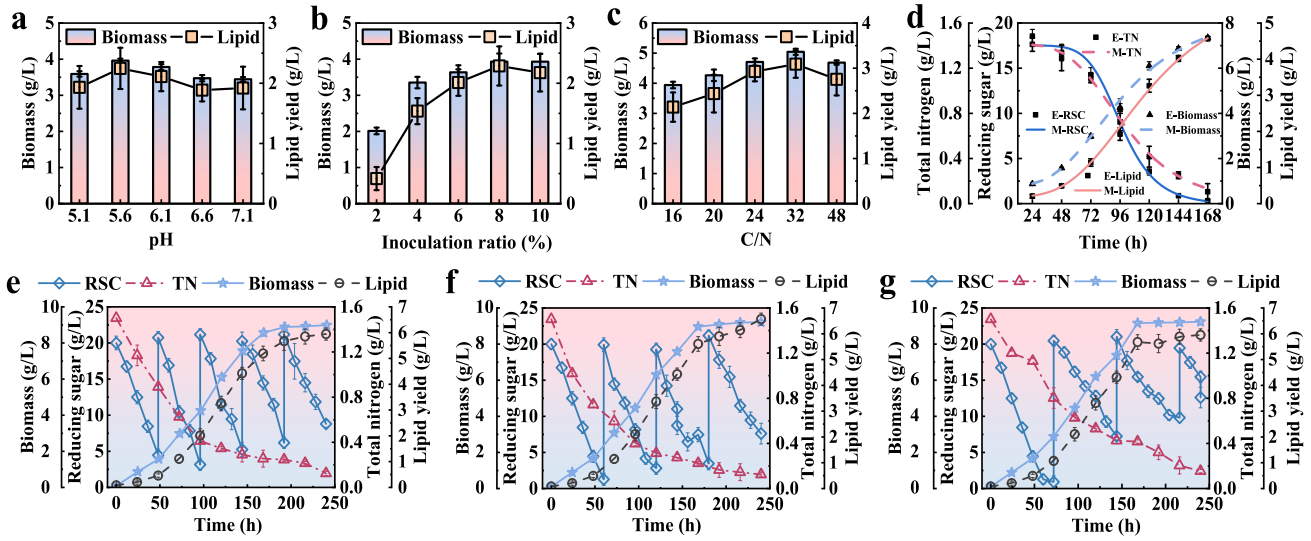

Fig. 5. Effects of fed-batch fermentation cultivation mode the biomass and lipid yield of *SnRK2*-14-OCS. pH, inoculation ratio, and C/N ratio on the biomass and lipid yield of *SnRK2*-14-OCS under batch cultivation mode (a-c); The fitting between experimental results (full line) and predicted values (dashed line) of biomass and lipid yield of *SnRK2*-14-OCS under the optimal batch conditions (d); Time course profiles of biomass and lipid yield of *SnRK2*-14-OCS at 48-h, 60-h, and 72-h fed-batch feeding interval with glucose supplementation (e-f). Data were presented as means of three biological replicates ± SD.

2.13-fold more than 48 h feeding interval and batch feeding mode (Fig. 5f). Additionally, the utilization rate of RSC reached 90.55 %, reflecting that *SnRK2*-14-OCS could effectively utilize RSC to support the growth and lipid biosynthesis under 60 h interval supplementation. However, it could be seen from Fig. 5f that TN concentration showed slight increase at fed-batch fermentation terminal. This might be due to that algal cells released nitrogen substances into culture system in fermentation process consequently enhanced TN concentration [57]. Therefore, TN consumption rate (87.69 %) was also lower than that of 48 h feeding interval. Whilst 72 h feeding interval achieved the highest biomass and lipid yield by 8.17 g/L and 4.95 g/L, which was higher than that batch fermentation mode but lower than 48 h and 60 h feeding interval (Fig. 5g). And the consumption rate of RSC (75.44 %) also exhibited reduction tendency by 72 h feeding interval than that of 48 h and 60 h interval. But the TN consumption rate (89.69 %) by 72 h feeding interval was between 48 h and 60 h interval. The aforementioned results indicated that the optimal fed-batch fermentation mode was closely-related to feeding frequency and feeding interval of supplements. Whereas *SnRK2*-14-OCS could operate well under fed-batch fermentation mode by 60 h feeding interval and further boosted biomass and lipid yield.

3.5. *SnRK2-14 overexpression upgraded biodiesel properties by regulating fatty acid profiles*

It was well-known that the fatty acid profiles could greatly affect algae-based biodiesel properties [58,59]. Therefore, the fatty acid profiles of the constructed *SnRK2*-14-OCS were examined to determine the suitability in refining high-quality biodiesel. As summarized in Table 1, regardless of *SnRK2*-14-OCS or WT, no significant discrepancy in fatty acid profiles were detected, being mainly composed of C16-C18 ranging from 92.85 % to 94.41 % as well as a small portion of above C20 and below C16 fatty acids. Among these fatty acids, palmitic acid (C16:0) and oleic acid (C18:1) were preponderant components followed by linoleic acid (C18:2) and then linolenic acid (C18:3) in both strain cells. This showed consistence with previous report where C16:0, C18:1, C18:2 and C18:3 fatty acids were dominant in *C. subellipsoidea* and the high proportion of C16-C18 were also desirable as preferable feedstock for high-quality biodiesel [2].

Excluding these mutual characteristics in both cell lines, *SnRK2*-14 overexpression also triggered some notable features in fatty acid profiles

Table 1
Fatty acid profiles in lipids of *SnRK2*-14 overexpression *C. subllipsoidea* strain.

Fatty acids profiles	Relative content (%)	
	WT	*SnRK2*-14-OCS
Lauric acid (C12:0)	0.03 ± 0.01	0.04 ± 0.01
Myristic acid (C14:0)	0.12 ± 0.04	0.15 ± 0.02
Pentadecanoic acid (C15:0)	0.20 ± 0.06	0.21 ± 0.08
Palmitic acid (C16:0)	31.36 ± 0.12	14.27 ± 0.13**
Palmitoleic acid (C16:1)	0.09 ± 0.01	0.13 ± 0.03
Heptadecanoic acid (C17:0)	0.10 ± 0.03	0.11 ± 0.05
Stearic acid (C18:0)	0.83 ± 0.12	0.78 ± 0.19
Oleic acid (C18:1)	32.86 ± 0.22	56.27 ± 0.17**
Linoleic acid (C18:2)	14.17 ± 0.14	12.09 ± 0.22*
α-Linolenic acid (C18:3)	13.44 ± 0.35	12.76 ± 0.23
Arachidic acid (C20:0)	0.06 ± 0.03	0.06 ± 0.01
Eicosenoic acid (C20:1)	1.51 ± 0.02	2.17 ± 0.07
Eicosadienoic acid (C20:2)	0.31 ± 0.12	0.33 ± 0.18
Eicosenoic acid (C20:1n9)	2.81 ± 0.30	1.26 ± 0.09
Behenic acid (C22:0)	0.11 ± 0.02	0.11 ± 0.08
Eicosatrienoic acid (C20:3)	0.22 ± 0.16	0.20 ± 0.13
Arachidonic acid (C20:4)	0.17 ± 0.04	0.11 ± 0.05
Tricosanoic acid (C23:0)	0.14 ± 0.06	0.07 ± 0.01
Lignoceric acid (C24:0)	1.45 ± 0.32	0.83 ± 0.27
Nervonic acid (C24:1)	0.05 ± 0.12	0.05 ± 0.04
Σ C16 + C18	92.85 ± 0.19	94.41 ± 0.16
Σ SFA	34.40 ± 1.20	16.63 ± 0.32**
Σ MUFA	37.32 ± 1.52	57.88 ± 3.37**
Σ PUFA	28.28 ± 0.93	25.49 ± 3.82

SFA, MUFA, and PUFA separately indicated saturated fatty acids, monounsaturated fatty acids, and polyunsaturated fatty acids. *SnRK2*-14-OCS and WT represented *SnRK2*-14 overexpression *C. subllipsoidea* strain and wild type strain, respectively. Data were presented as means of three biological replicates ± SD.

of *SnRK2*-14-OCS, including 1) C16:0 content (14.27 %) showed 2.20-fold reduction than that of WT, indicating good fluidity of *SnRK2*-14-OCS fatty acids-based biodiesel under low temperature [60]; 2) C18:1 accounted for 56.27 % of TFAs and this proportion represented 1.71-fold more than that of WT. The elevated level of C18:1 could endow biodiesel with a low melting point [60]; 3) C18:2 content (12.09 %) showed significant down-regulation than in WT (14.17 %) ($p < 0.05$). This was beneficial in promoting discharge performance and oxidation stability of *SnRK2*-14-OCS while maintaining acceptable low temperature operation [2]; 4) C18:3 content occupied 12.76 % of TFAs, which more easily

met the biodiesel specifications (<12 %) established by ASTM D-6751 and DINV 14214; 5) The proportion of monounsaturated fatty acids (MUFAs) (57.88 %) exceeded the summed proportion (42.12 %) of saturated fatty acids (SFAs) (16.63 %) and polyunsaturated fatty acids (PUFAs) (25.49 %). Whereas the percentage of MUFAs (37.32 %) in WT was lower than the sum (62.68 %) of SFAs (34.40 %) and PUFAs (28.28 %). Usually, lipids dominated by MUFAs tended to have superior oxidation stability and reduced viscosity for alga-based biodiesel [25]. These results indicated that *SnRK2*-14 overexpression regulated the fatty acid profiles in *SnRK2*-14-OCS and could target high-quality biodiesel.

To further verify the feasibility of fatty acid profiles of *SnRK2*-14-OCS for high-quality biodiesel, the theoretical values of fuel properties involving in CN, IV, υi, ρ, CP, CFPP, ADU, LCSF, HHV, and Y were calculated and summarized in Table 2. Table 2 revealed that CN value of *SnRK2*-14-OCS was 55.87, which was higher than that of WT (54.42) and also showed compliance with the minimum CN prescription of 51 and 47 by EN 14214 and ASTM D6751 standards. Whilst IV was 90.83 g I_2 100/g oil and showed reduction than that of WT (107.00 g I_2 100/g oil). This was also coincident with EN standards where IV was less than 120 g I_2 100/g oil. The previous report indicated that a relatively-high CN and a relatively-lower IV were beneficial for ignition quality and oxidation stability of biodiesel [61]. Therefore, CN and IV of *SnRK2*-14-OCS-based biodiesel not only accorded with EN and ASTM standards but also more endowed biodiesel with the superior ignition quality and oxidation stability than WT. Additionally, CP and CFPP parameters could be used to express cold flow performance of biodiesel. Whereas CFPP was interrelated with the LCSF. In this study, CP and CFPP values of *SnRK2*-14-OCS and WT were between 15.74 and 16.47 °C and −16.39 to −16.41 °C, respectively. LCSF values were separately 0.03 and 0.02 in *SnRK2*-14-OCS- and WT-based biodiesel. These parameters of *SnRK2*-14-OCS-based biodiesel were in the range of EN standards (CP>4 and $-20 \leq$ CFPP ≤ 5 ℃) and indicated the desirable characteristic of having a lower CFPP and feasible applications under colder climates [62]. Biodiesel quality could be also described by *νi* parameter, which was associated with fuel combustion, vaporization, and atomization [58]. However, the range of acceptable *νi* in EN standard was narrow (3.5–5.0 mm^2/s) while ASTM standard permitted a wider range of acceptable *νi* value (1.9–6.0 mm^2/s). Interestingly, the *νi* value of *SnRK2*-14-OCS-based biodiesel was calculated to be 4.41 mm^2/s, which easily agreed with EN and ASTM standards and reflected superior flow characteristics of biodiesel against resistance [58]. Synchronously, the *ρ* value was also included as a specification in ASTM (0.878 $g{\cdot}m^3$) and EN (0.86–0.90 $g{\cdot}m^3$) standards. Whereas *ρ* value (0.88 $g{\cdot}m^3$) of *SnRK2*-14-OCS-based biodiesel also fall within the two criteria to indicate the effortless transportability of this biodiesel [62]. When compared to ASTM standard for HHV (≥35 MJ/kg), the HHV value (40.77 MJ/kg) of *SnRK2*-14-OCS-based biodiesel was also acceptable since the high HHV in such fuel could completely combust to release more heat. Oxidation stability associated with sediments, resins, and acids formation was another very important parameter related to the storage of biodiesel. Oxidation stability for EN standard should be ≥ 6 h at 110 °C. Whereas Y value (6.87 h) of *SnRK2*-14-OCS-based biodiesel was slightly higher than that standard, indicating it was stable response to oxidative stress. Additionally, although no standardized ADU parameter in EN and AST, the ADU of *SnRK2*-14-OCS-based biodiesel was lower than that of WT, indicating the stability of *SnRK2*-14-OCS-based biodiesel was more preferable than WT. Overall, the generated fatty acid profiles in *SnRK2*-14-OCS could be considered as potential feedstock to benefit biodiesel properties.

It could be also found in previous reports that vegetable oils-based biodiesel was potential fuels since possessing key characteristics such as biodegradability, lubricating properties, the ability to mix with petroleum diesel in any ratio, and a higher cetane number compared to petrochemical diesel [62]. However, the fuel properties *SnRK2*-14-OCS-based biodiesel in this study presented many advantages compared to conventional vegetable oils-based biodiesel. Specifically, the *νi* value of *SnRK2*-14-OCS-based biodiesel was lower than that range of 4 ~ 5 mm^2/s of vegetable oils-based biodiesel to preferably support flow against resistance; the high CP value exceeded soybean oil- and cuphea oil-based biodiesel (separately the range of 1 °C to −2 °C and −9 °C to −10 °C) but was basically-equivalent to *Moringa oleifera* oil-based biodiesel (18 °C) to indicate it's operability of low temperature applications [63]; the current HHV value (40.77 MJ/kg) of *SnRK2*-14-OCS-based biodiesel was also comparable with the HHV of commercial petro-diesel (44.8 MJ/kg), vegetable oils-based (39.3 ~ 41.27 MJ/kg), and other algae-based biodiesel (35.3 ~ 41.2 MJ/kg) [62]. It was worth mentioned that *SnRK2*-14-OCS-based biodiesel appeared more susceptible to oxidation due to the relative high amounts of linoleate and linolenate in fatty acid profiles than most vegetable oils (Table 1). However, the results in Table 2 seemed to imply that the oxidation stability of *SnRK2*-14-OCS-based biodiesel met with EN and ASTM standards even was better than that of WT. This might be due to that *SnRK2* overexpression eliminated ROS and elevated the T-AOC of *SnRK2*-14-OCS to prevent PUFAs peroxidation consequently upgraded the quality of biodiesel (Fig. 4). But such effects did not completely inhibit the oxidation of FAs and biodiesel. Therefore, some investigations proposed that extra antioxidant supplementation were the most common way of improving the oxidative stability of biodiesel [63]. Actually, as insufficient quantities of alga-based biodiesel were available, little information on antioxidants applications in actual algal biodiesel were traceable. A thematic study on simulating algal biodiesel indicated that *tert*-butylhydroquinone might be effective in preventing biodiesel oxidation, but needed verifications on actual algal biodiesel fuels [63]. Additionally, an important imagine was that many antioxidant factors in algal residue after extracting fatty acids for biodiesel could be exploited into the oxidation stability of alga-based biodiesel.

Even though the above clues indicated the potencies of *SnRK2*-14 overexpression in improving the lipid production performances of *SnRK2*-14-OCS and upgrading biodiesel quality, but *SnRK2*-14-OCS in industrial size applications needed to solve low cost-efficiency scale-up culture, microorganisms contamination, and seasonal conditions limitation [64]. Therefore, needing to carefully consider and monitor the growth parameters of *SnRK2*-14-OCS in the mass cultivation of biomass. For the photo-bioreactor, prior to mass cultivation, a lab-scale pilot plant run was important. Whereas in the raceway pond, some factor such

Table 2
The fuel properties of *SnRK2*-14-OCS fatty acids-based biodiesel.

Biodiesel parameters	Units	Strains WT	*SnRK2*-14-OCS	ASTM D6751	DIN EN 14214
Average degree of unsaturation (ADU)	–	1.27	1.05	NA	NA
Cetane number (CN)	–	54.42	55.87	≥47	≥51
Iodine value (IV)	g I_2 100/g oil	107.00	90.83	NA	≤120
Kinematic viscosity (*νi*)	mm^2/s	4.54	4.41	1.9–6.0	3.5–5.0
Specific gravity (*ρ*)	$g{\cdot}m^3$	0.88	0.88	0.878	0.86–0.90
Cloud point (CP)	℃	15.74	16.47	NA	>4
Long chain saturation factor (LCSF)	wt %	0.03	0.02	NA	NA
Higher heating value (HHV)	MJ/kg	40.38	40.77	NA	≥35
Cold filter plugging point (CFPP)	℃	−16.39	−16.41	NA	≤5 ≥ -20
Oxidation stability (Y)	h	6.41	6.87	NA	≥6

Note: NA presented without specifications. ASTM D-6751 and DINV 14214 indicated American Society for Testing and Materials and also Deutsches Institut für Normung biodiesel standards.

as light intensity, spectral quality, temperature, photoperiod, microbial invasion could not be controlled and were prone to environmental fluctuation. Parameters associated with raceway pond such as paddle-wheel speed and impeller speed would affect the quality and quantity of biomass production [65]. Therefore, *SnRK2*-14-OCS strain was required to be well adapted or domesticated by the temperature, light, pH, oxygen concentration of the condition in which it was cultivated to yield high biomass. Additionally, the overall cost of the mass production process should be monitored in terms of nutrients and energy supply. In this regard, using low-cost industrial or agricultural waste or sludge for the cultivation of microalgae were proved to be theoretically feasible [66]. And optimizing biodiesel production from waste with computational chemistry, machine learning, and policy insights were also recommended [67]. Integrating the major goals of *SnRK2*-14-OCS-based biodiesel production with co-production of high-value by-products such as proteins and polysaccharide-rich streams of de-oiled algal biomass and natural pigments were also important interventions to ensure the cost-competitiveness of the production process [68]. Collectively, efficient resources selection and consideration of multiple value chains were essential to augment economic feasibility of *SnRK2*-14-OCS-based biodiesel production.

4. Conclusion

This study firstly unraveled the lipid elevating efficacy and biodiesel upgrade by *SnRK2*-14 homologous overexpression in *C. subllipsoidea* and also provided a new functional gene in constructing robust strain for industrial and sustainable biodiesel production. The overarching impact of *SnRK2*-14 overexpression on lipid accumulation were to up-regulate lipid-related genes, transfer intermediates or energy from carbohydrate/protein degradation into lipid pathway, and also strengthen total antioxidant capacity in engineered microalgae. However, *SnRK2*-14 engineering microalgae efforts including low-cost scale-up culture, micro-organisms contamination, seasonal conditions and variations, downstream processing, and complicated operation and monitoring of the whole system ought to be devoted into biodiesel production pipelines.

CRediT authorship contribution statement

Yuanyuan Luo: Writing – original draft, Visualization, Investigation. **Sisi Zhao:** Formal analysis, Data curation. **Zhixuan Fan:** Formal analysis, Data curation. **Yuqin Li:** Writing – review & editing, Supervision, Resources, Funding acquisition, Conceptualization. **Zongfan Peng:** Formal analysis, Data curation. **Yulong Zhang:** Formal analysis, Data curation. **Siran Feng:** Writing – review & editing. **Jinhua Mou:** Writing – review & editing. **Zhenyao Wang:** Writing – review & editing, Supervision. **Carol Sze Ki Lin:** Writing – review & editing. **Xuan Li:** Writing – review & editing.

Declaration of competing interest

The authors declare that they have no known competing financial interests or personal relationships that could have appeared to influence the work reported in this paper.

Acknowledgements

This work is supported by the Natural Science Foundation of Hunan Province (2024JJ7548) and the National Natural Science Foundation of China (21676228).

Appendix A. Supplementary data

Supplementary data to this article can be found online at https://doi.org/10.1016/j.cej.2025.159607.

Data availability

Data will be made available on request.

References

[1] A. Brar, M. Kumar, T. Soni, V. Vivekanand, N. Pareek, Insights into the genetic and metabolic engineering approaches to enhance the competence of microalgae as biofuel resource: a review, Bioresour. Technol. 339 (2021) 125597, https://doi.org/10.1016/j.biortech.2021.125597.
[2] Y.Q. Li, Y.Y. Luo, R. Zhou, X.H. Zuo, Y. Zhang, Z.Y. Wang, X. Li, X. Zhang, Z. Qin, C. S.K. Lin, Coculture of *Chlorella protothecoides* and *Coccomyxa subellipsoidea* enhances cell growth and lipid accumulation: an effective strategy for biodiesel production, Chem. Eng. J. 486 (2024) 150302, https://doi.org/10.1016/j.cej.2024.150302.
[3] K. Gaurav, K. Neeti, R. Singh, Microalgae-based biodiesel production and its challenges and future opportunities: a review, Green Technol. Sustain. 2 (2024) 100060, https://doi.org/10.1016/j.grets.2023.100060.
[4] X.T. Song, F.Y. Kong, B.F. Liu, Q.Q. Song, N.Q. Ren, H.Y. Ren, Lipidomics analysis of microalgal lipid production and heavy metal adsorption under glycine betaine-mediated alleviation of low-temperature stress, J. Hazard. Mater. 480 (2024) 135831, https://doi.org/10.1016/j.jhazmat.2024.135831.
[5] K. Ramphal, A. Lewis, N.A. Trzaskalski, A. Kisiala, E.N. Morrison, S.S. Narine, R.J. N. Emery, Phytohormonal impacts on fatty acid profiles in *Chlorella vulgaris* Beijerinck: endogenous identification and exogenous application of cytokinins and abscisic acid, J. Appl. Phycol. 35 (2023) 2205–2218, https://doi.org/10.1007/s10811-023-03068-y.
[6] X. Li, Y.Z. Lu, N. Li, Y.Z. Wang, R. Yu, G.C. Zhu, R.J. Zeng, Mixotrophic cultivation of microalgae using biogas as the substrate, Environ. Sci. Technol. 56 (2022) 3669–3677, https://doi.org/10.1021/acs.est.1c06831.
[7] K.S. Khoo, I. Ahmad, K.W. Chew, K. Iwamoto, A. Bhatnagar, P.L. Show, Enhanced microalgal lipid production for biofuel using different strategies including genetic modification of microalgae: a review, Prog. Energy Combust. Sci. 96 (2023) 101071, https://doi.org/10.1016/j.pecs.2023.101071.
[8] C.F. Muñoz, C. Südfeld, M.I.S. Naduthodi, R.A. Weusthuis, M.J. Barbosa, R. H. Wijffels, S. D'Adamo, Genetic engineering of microalgae for enhanced lipid production, Biotechnol. Adv. 52 (2021) 107836, https://doi.org/10.1016/j.biotechadv.2021.107836.
[9] Y. Shi, M.J. Liu, Y.F. Pan, H.H. Hu, J. Liu, Δ6 fatty acid elongase is involved in eicosapentaenoic acid biosynthesis via the ω6 pathway in the marine alga *Nannochloropsis oceanica*, J. Agric. Food Chem. 69 (2021) 9837–9848, https://doi.org/10.1021/acs.jafc.1c04192.
[10] X. Wang, Y.H. Liu, W. Wei, X. Zhou, W.S.Q. Yuan, S. Balamurugan, T.B. Hao, W. D. Yang, J.S. Liu, H.Y. Li, Enrichment of long-chain polyunsaturated fatty acids by coordinated expression of multiple metabolic modes in the oleaginous microalga *Phaeodactylum tricornutum*, J. Agric. Food Chem. 65 (2017) 7713–7720, https://doi.org/10.1021/acs.jafc.7b02397.
[11] J. Xue, S. Balamurugan, D.W. Li, Y.H. Liu, H. Zeng, L. Wang, W.D. Yang, J.S. Liu, H. Y. Li, Glucose-6-phosphate dehydrogenase as a target for highly efficient fatty acid biosynthesis in microalgae by enhancing NADPH supply, Metab. Eng. 41 (2017) 212–221, https://doi.org/10.1016/j.ymben.2017.04.008.
[12] M. La Russa, C. Bogen, A. Uhmeyer, A. Doebbe, E. Filippone, O. Kruse, J. H. Mussgnug, Functional analysis of three type-2 DGAT homologue genes for triacylglycerol production in the green microalga *Chlamydomonas reinhardtii*, J. Biotechnol. 162 (2012) 13–20, https://doi.org/10.1016/j.jbiotec.2012.04.006.
[13] R.P. Haslam, M.L. Hamilton, C.K. Economou, R. Smith, K.L. Hassall, J.A. Napier, O. Sayanova, Overexpression of an endogenous type 2 diacylglycerol acyltransferase in the marine diatom *Phaeodactylum tricornutum* enhances lipid production and omega-3 long-chain polyunsaturated fatty acid content, Biotechnol. Biofuels. 13 (2020) 87, https://doi.org/10.1186/s13068-020-01726-8.
[14] S. Singh, A. Singh, S. Singh, N. Prasad, P. Laxmi, R.K.A. Singh, IAA induced biomass and lipid overproduction in microalga via two-stage cultivation strategy: Characterization using FTIR/CHNS/TGA/DTG and 1H-NMR for bioenergy potential, Energy Convers. Manage. 311 (2024) 118546, https://doi.org/10.1016/j.enconman.2024.118546.
[15] R. Norlina, M.N. Norashikin, S.H. Loh, A. Aziz, T.S. Cha, Exogenous abscisic acid supplementation at early stationary growth phase triggers changes in the regulation of fatty acid biosynthesis in *Chlorella vulgaris* UMT-M1, Appl. Biochem. Biotechnol. 191 (2020) 1653–1669, https://doi.org/10.1007/s12010-020-03312-y.
[16] K. Ding, Z. Chen, Q.W. Wan, X.L. Hu, X.H. Wang, H. Li, Y.Z. Wang, Y. Luo, D. B. Xiang, Improving antistress capacity and lipid productivity in the green alga *Chlorella pyrenoidosa* by adding abscisic acid under salt stress conditions, Algae 39 (2024) 207–222, https://doi.org/10.4490/algae.2024.39.8.28.
[17] Y.H. Lin, Y. Dai, W.N. Xu, X.B. Wu, Y.Y. Li, H.M. Zhu, H.T. Zhou, The growth, lipid accumulation and fatty acid profile analysis by abscisic acid and indol-3-acetic acid induced in *Chlorella* sp. FACHB-8, Int. J. Mol. Sci. 23 (2022) 4064, https://doi.org/10.3390/ijms23074064.
[18] Q. Wang, S.Z. Fan, S.X. Liu, J.L. Xu, X.H. Li, A mutated algal species of *Isochrysis* sp. obtained via atmospheric room temperature plasma mutagenesis promoted lipid accumulation through the abscisic acid pathway, Algal Res., 82 (2024) 103675. https://doi.org/10.1016/j.algal.2024.103675.
[19] D. Fierli, M.E. Barone, V. Graceffa, N. Touzet, Cold stress combined with salt or abscisic acid supplementation enhances lipogenesis and carotenogenesis in

Phaeodactylum tricornutum (Bacillariophyceae), Bioprocess Biosyst. Eng. 45 (2022) 1967–1977, https://doi.org/10.1007/s00449-022-02800-1.
[20] Z. Lin, Y. Li, Y.B. Wang, X.L. Liu, L. Ma, Z.J. Zhang, C. Mu, Y. Zhang, L. Peng, S. J. Xie, C.P. Song, H.Z. Shi, J.K. Zhu, P.C. Wang, Initiation and amplification of SnRK2 activation in abscisic acid signaling, Nat. Commun. 12 (2021) 2456, https://doi.org/10.1038/s41467-021-22812-x.
[21] Y.F. Zhu, P.C. Huang, P.C. Guo, L. Chong, G.B. Yu, X.L. Sun, T. Hu, Y. Li, C.C. Hsu, K. Tang, Y. Zhou, C.Z. Zhao, W. Gao, W.A. Tao, T. Mengiste, J.K. Zhu, CDK8 is associated with RAP2.6 and SnRK2.6 and positively modulates abscisic acid signaling and drought response in *Arabidopsis*, New Phytol. 228 (2020) 1573–1590, https://doi.org/10.1111/nph.16787.
[22] M.J. Zhang, L. Liu, C.X. Chen, Y. Zhao, C.H. Pang, M. Chen, Heterologous expression of a Fraxinus velutina SnRK2 gene in *Arabidopsis* increases salt tolerance by modifying root development and ion homeostasis, Plant Cell Rep. 41 (2022) 1895–1906, https://doi.org/10.1007/s00299-022-02899-2.
[23] L.C. Zhu, Y.Z. Li, C.C. Wang, Z.Q. Wang, W.J. Cao, J. Su, Y.J. Peng, B.Y. Li, B. Q. Ma, F.W. Ma, Y.L. Ruan, M.J. Li, The SnRK2.3-AREB1-TST1/2 cascade activated by cytosolic glucose regulates sugar accumulation across tonoplasts in apple and tomato, Nat. Plants. 9 (2023) 951–964, https://doi.org/10.1038/s41477-023-01443-8.
[24] D.J. Xiang, L.L. Man, S. Cao, P. Liu, Z.G. Li, X.D. Wang, Ectopic expression of an oat *SnRK2* Gene, *AsSnRK2D*, enhances dehydration and salinity tolerance in tobacco by modulating the expression of stress-related genes, Braz. J. Bot. 43 (2020) 429–446, https://doi.org/10.1007/s40415-020-00614-7.
[25] Y.Q. Li, Y.Y. Luo, Z.Y. Wang, S. Zou, X. Meng, X. Liu, Enhancement of carbon bio-fixation and lipid accumulation in *Coccomyxa subellipsoidea* with triethanolamine CO_2 absorbent manipulation, Biochem. Eng. J. 198 (2023) 109018, https://doi.org/10.1016/j.bej.2023.109018.
[26] K.Y. Lu, Y.H. Song, W.J. Jin, F.Z. Wang, L. Chen, W.W. Zhang, Increased growth and fatty acid accumulation via overexpression of hypothetical protein Unigene 12362 with the SWIB/MDM2 domain in *Schizochytrium*, Chem. Eng. J. 493 (2024) 152689, https://doi.org/10.1016/j.cej.2024.152689.
[27] P. Shirazian, M. Azin, A. Bozorg, Kinetic models to describe *Nannochloropsis salina* cultivation under different illumination conditions, Environ. Prog. Sustainable Energy. 41 (2022) e13833, https://doi.org/10.1002/ep.13833.
[28] Y.A. Bai, Y.Q. Li, Y.F. Tang, R. Zhou, Y.W. Fan, *Rhizopus oryzae* fermentation wastewater nutrient removal coupling protein fodder production by employing *Chlorella pyrenoidosa*, Bioresour. Technol. 362 (2022) 127858, https://doi.org/10.1016/j.biortech.2022.127858.
[29] Z.Y. Yang, K.X. Huang, Y.R. Zhang, L. Yang, J.L. Zhou, Q. Yang, F. Gao, Efficient microalgal lipid production driven by salt stress and phytohormones synergistically, Bioresour. Technol. 367 (2023) 128270, https://doi.org/10.1016/j.biortech.2022.128270.
[30] D. Fierli, M.E. Barone, A. Mc Donnell, T. Conlon, N. Touzet, Combined application of exogenous phytohormones and blue light illumination to the marine diatom *Phaeodactylum tricornutum*, Algal Res. 71 (2023) 103052, https://doi.org/10.1016/j.algal.2023.103052.
[31] T.A. Kozlova, A.V. Kartashov, E. Zadneprovskaya, A. Krapivina, P. Zaytsev, O. B. Chivkunova, A.E. Solovchenko, Effect of abscisic acid on growth, fatty acid profile, and pigment composition of the Chlorophyte *Chlorella (Chromochloris) zofingiensis* and its co-culture microbiome, Life. 13 (2023) 452, https://doi.org/10.3390/life13020452.
[32] G.V. Novikova, A.V. Nosov, N.S. Stepanchenko, A.A. Fomenkov, A.S. Mamaeva, I. E. Moshkov, Plant cell proliferation and its regulators, Russ. J. Plant Physiol. 60 (2013) 500–506, https://doi.org/10.1134/S1021443713040109.
[33] W.A. Stirk, P. Bálint, D. Tarkowská, O. Novák, G. Maróti, K. Ljung, V. Turecková, M. Strnad, V. Ördög, J. van Staden, Effect of light on growth and endogenous hormones in *Chlorella minutissima* (Trebouxiophyceae), Plant Physiol. Biochem. 79 (2014) 66–76, https://doi.org/10.1016/j.plaphy.2014.03.005.
[34] T.T. Liu, F. Liu, C. Wang, Z.Y. Wang, Y.Q. Li, The boosted biomass and lipid accumulation in *Chlorella vulgaris* by supplementation of synthetic phytohormone analogs, Bioresour. Technol. 232 (2017) 44–52, https://doi.org/10.1016/j.biortech.2017.02.004.
[35] G.L. Xing, H.L. Yuan, J.S. Yang, J.Y. Li, Q.X. Gao, W.L. Li, E.T. Wang, Integrated analyses of transcriptome, proteome and fatty acid profilings of the oleaginous microalga *Auxenochlorella protothecoides* UTEX 2341 reveal differential reprogramming of fatty acid metabolism in response to low and high temperatures, Algal Res. 33 (2018) 16–27, https://doi.org/10.1016/j.algal.2018.04.028.
[36] X.Y. Wei, Y.Z. Wang, X.E. Liu, Z.J. Hu, J.Y. Qian, T.Q. Shi, Y.T. Wang, C. Ye, Metabolic analysis of *Schizochytrium* sp. mutants with high EPA content achieved with ARTP mutagenesis screening, Bioprocess Biosyst. Eng. 46 (2023) 893–901, https://doi.org/10.1007/s00449-023-02874-5.
[37] S.T. Gumbi, A. Kumar, A.O. Olaniran, Lipid productivity and biosynthesis gene response of indigenous microalgae *Chlorella* sp. T4 strain for biodiesel production under phosphorus load, BioEnergy Res. 15 (2022) 2090–2101, https://doi.org/10.1007/s12155-022-10419-z.
[38] W.F. Guo, Y.W. Weng, W.K. Ma, C.F. Chang, Y.Q. Gao, X.G. Huang, F. Zhang, Improving lipid content in the diatom *Phaeodactylum tricornutum* by the knockdown of the enoyl-CoA hydratase using CRISPR interference, Curr. Issues Mol. Biol. 46 (2024) 10923–10933, https://doi.org/10.3390/cimb46100649.
[39] M.M. Hasan, X.D. Liu, M. Waseem, G.Q. Yao, N.M. Alabdallah, M.S. Jahan, X. W. Fang, ABA activated SnRK2 kinases: an emerging role in plant growth and physiology, Plant Signaling Behav. 17 (2022) e2071024, https://doi.org/10.1080/15592324.2022.2071024.
[40] A.K. Bajhaiya, A.P. Dean, T. Driver, D.K. Trivedi, N.J.W. Rattray, J.W. Allwood, R. Goodacre, J.K. Pittman, High-throughput metabolic screening of microalgae genetic variation in response to nutrient limitation, Metabolomics 12 (2016) 9, https://doi.org/10.1007/s11306-015-0878-4.
[41] D. Unal, F.O. Cekic, Cold acclimation of SnRK2.2 kinases mutant *Chlamydomonas reinhardtii*, Phycol. Res. 67 (2019) 202–207, https://doi.org/10.1111/pre.12371.
[42] K. Takahashi, Y. Ide, J. Hayakawa, Y. Yoshimitsu, I. Fukuhara, J. Abe, Y. Kasai, S. Harayama, Lipid productivity in TALEN-induced starchless mutants of the unicellular green alga *Coccomyxa* sp. strain Obi, Algal Res. 32 (2018) 300–307, https://doi.org/10.1016/j.algal.2018.04.020.
[43] B. Tzovaras, F. Segers, A. Bicker, F. Dal Grande, J. Otte, S. Anvar, T. Hankeln, I. Schmitt, I. Ebersberger, What is in Umbilicaria Pustulata? A metagenomic approach to reconstruct the holo-genome of a lichen, Genome Biol. Evol. 12 (2020) 309–324, https://doi.org/10.1093/gbe/evaa049.
[44] M.R. Jia, X.L. Li, W. Wang, T.Y. Li, Z.R. Dai, Y.T. Chen, K.K. Zhang, H.C. Zhu, W. W. Mao, Q.Q. Feng, L.P. Liu, J.Q. Yan, S.L. Zhong, B.B. Li, W.S. Jia, SnRK2 subfamily I protein kinases regulate ethylene biosynthesis by phosphorylating HB transcription factors to induce *ACO1* expression in apple, New Phytol. 234 (2022) 1262–1277, https://doi.org/10.1111/nph.18040.
[45] X. Wang, Q. Tang, F.M. Chi, H.D. Liu, H.J. Zhang, Y. Song, Sucrose hon-fermenting1-related protein kinase VcSnRK2.3 promotes anthocyanin biosynthesis in association with VcMYB1 in blueberry, Front. Plant Sci. 14 (2023) 1018874, https://doi.org/10.3389/fpls.2023.1018874.
[46] D.K. Yadav, M. Yadav, P. Rani, A. Yadav, N. Bhardwaj, N.R. Bishnoi, A. Singh, Screening of best growth media for *Chlorella vulgaris* cultivation and biodiesel production, Biofuels 15 (2024) 271–277, https://doi.org/10.1080/17597269.2023.2235787.
[47] Y.T. Zhao, D.F. Li, J.W. Xu, P. Zhao, T. Li, H.X. Ma, X.Y. Yu, Melatonin enhances lipid production in *Monoraphidium* sp QLY-1 under nitrogen deficiency conditions via a multi-level mechanism, Bioresour. Technol. 259 (2018) 46–53, https://doi.org/10.1016/j.biortech.2018.03.014.
[48] D.J. Xiang, L.L. Man, S. Cao, P. Liu, Z.G. Li, X.D. Wang, Heterologous expression of an *Agropyron cristatum* SnRK2 protein kinase gene (*AcSnRK2.11*) increases freezing tolerance in transgenic yeast and tobacco, 3 Biotech. 10 (2020) 209, https://doi.org/10.1007/s13205-020-02203-7.
[49] Y. Yuan, T.T. Zhao, W.Z. Gao, W.Q. Ye, Y.L. Chen, D.Z. Sun, Z. Zhang, Reactive oxygen species derived from NADPH oxidase as signaling molecules regulate fatty acids and astaxanthin accumulation in *Chromochloris zofingiensis*, Front. Microbiol. 15 (2024) 1387222, https://doi.org/10.3389/fmicb.2024.1387222.
[50] N. Esim, P. Dawar, N.P. Arslan, T. Orak, M. Doymus, F. Azad, S. Ortucu, S. Albayrak, M. Taskin, Natural metabolites with antioxidant activity from micro- and macro-algae, Food Biosci. 62 (2024) 105089, https://doi.org/10.1016/j.fbio.2024.105089.
[51] X.T. Song, F.Y. Kong, B.F. Liu, Q.Q. Song, N.Q. Ren, H.Y. Ren, Antioxidants alleviated low-temperature stress in microalgae by modulating reactive oxygen species to improve lipid production and antioxidant defense, Bioresour. Technol. 413 (2024) 131451, https://doi.org/10.1016/j.biortech.2024.131451.
[52] M. Almendinger, F. Saalfrank, S. Rohn, E. Kurth, M. Springer, D. Pleissner, Characterization of selected microalgae and cyanobacteria as sources of compounds with antioxidant capacity, Algal Res. 53 (2021) 102168, https://doi.org/10.1016/j.algal.2020.102168.
[53] I. Telussa, Rusnadi, Z. Nurachman, Dynamics of β-carotene and fucoxanthin of tropical marine *Navicula* sp. as a response to light stress conditions, Algal Res. 41 (2019) 101530, https://doi.org/10.1016/j.algal.2019.101530.
[54] I.D.B. Moussa, M.A. Masmoudi, S. Choura, M. Chamkha, S. Sayadi, Extraction optimization using response surface methodology and evaluation of the antioxidant and antimicrobial potential of polyphenols in *Scenedesmus* sp. and *Chlorella* sp, Biomass Convers. Biorefin. 13 (2023) 7185–7198, https://doi.org/10.1007/s13399-021-01850-x.
[55] X.T. Song, B.F. Liu, F.Y. Kong, Q.Q. Song, N.Q. Ren, H.Y. Ren, Lipid accumulation by a novel microalga *Parachlorella kessleri* R-3 with wide pH tolerance for promising biodiesel production, Algal Res. 69 (2023) 102925, https://doi.org/10.1016/j.algal.2022.102925.
[56] B.T. Dang, T.T. Nguyen, H.H. Ngo, M.D.T. Pham, L.T. Le, N.K.Q. Nguyen, T.D. H. Vo, S. Varjani, S.J. You, K.A. Lin, K.P.H. Huynh, X.T. Bui, Influence of C/N ratios on treatment performance and biomass production during co-culture of microalgae and activated sludge, Sci. Total Environ. 837 (2022) 155832, https://doi.org/10.1016/j.scitotenv.2022.155832.
[57] C. Li, J.X. Wang, J.H. Wang, Z.Y. Chi, Effects of staged multiple phytohormones application on capillary-driven attached *Chlorella* sp. biofilm, J. Environ. Manage. 351 (2024) 119886, https://doi.org/10.1016/j.jenvman.2023.119886.
[58] R.K. Bharti, C. Kaushal, A. Singh, D.W. Dhar, R. Babu, A. Kaushik, Evaluation of fuel properties for possible biodiesel output based on the fatty acid composition of oleaginous plants and microalgae, Sci. Total Environ. 918 (2024) 170448, https://doi.org/10.1016/j.scitotenv.2024.170448.
[59] Q.T. Wang, Y.B. Feng, Y.D. Lu, Y. Xin, C. Shen, L. Wei, Y.X. Liu, N.N. Lv, X.F. Du, W.Q. Zhu, B.R. Jeong, S. Xue, J. Xu, Manipulating fatty-acid profile at unit chain-length resolution in the model industrial oleaginous microalgae *Nannochloropsis*, Metab. Eng. 66 (2021) 157–166, https://doi.org/10.1016/j.ymben.2021.03.015.
[60] S.M. Xu, S. Gao, Y.F. An, Research progress of engineering microbial cell factories for pigment production, Biotechnol. Adv. 65 (2023) 108150, https://doi.org/10.1016/j.biotechadv.2023.108150.
[61] M.E.H. Osman, A.M. Abo-Shady, S.F. Gheda, S.M. Desoki, M.E. Elshobary, Unlocking the potential of microalgae cultivated on wastewater combined with salinity stress to improve biodiesel production, Environ. Sci. Pollut. Res. 30 (2023) 114610–114624, https://doi.org/10.1007/s11356-023-30370-6.
[62] H.Y. Wang, X.J. Hu, C. Shao, M. Elshobary, F.F. Zhu, Y. Cui, C.S. Zhang, J.H. Ni, S. H. Huo, Optimizing mixotrophic cultivation of oil-rich *Tribonema minus* using

volatile fatty acids and glycerin: A promising approach for pH-controlling and enhancing lipid productivity, J. Cleaner Prod. 402 (2023) 136733, https://doi.org/10.1016/j.jclepro.2023.136733.
[63] A. Ijaz, Z. Anwar, M. Zafar, Screening of wastewater *Oedogonium oblangum* algae for hyper-oil transformation into biodiesel by response surface methodology, Kuwait J. Sci. 50 (2023) 627–638, https://doi.org/10.1016/j.kjs.2023.03.005.
[64] K.S.H. Eldiehy, P. Bardhan, D. Borah, M. Gohain, M.A. Rather, D. Deka, M. Mandal, A comprehensive review on microalgal biomass production and processing for biodiesel production, Fuel 324 (2022) 124773, https://doi.org/10.1016/j.fuel.2022.124773.
[65] S.M. Rahul, M.A. Sundaramahalingam, C.S. Shivamthi, R.S. Kumar, P. Varalakshmi, S. Karthikumar, J. Kanimozhi, R.V. Kumar, S. Sabarathinam, I. G. Moorthy, A. Pugazhendhi, Insights about sustainable biodiesel production from microalgae biomass: A review, Int. J. Energy Res. 45 (2021) 17028–17056, https://doi.org/10.1002/er.6138.
[66] J. Marousek, A. Marousková, B. Gavurová, D. Tucek, O. Strunecky, Competitive algae biodiesel depends on advances in mass algae cultivation, Bioresour. Technol. 374 (2023) 128802, https://doi.org/10.1016/j.biortech.2023.128802.
[67] A.I. Osman, M. Nasr, M. Farghali, A.K. Rashwan, A. Abdelkader, A.H. Al-Muhtaseb, I. Ihara, D.W. Rooney, Optimizing biodiesel production from waste with computational chemistry, machine learning and policy insights: a review, Environ. Chem. Lett. 22 (2024) 1005–1071, https://doi.org/10.1007/s10311-024-01700-y.
[68] S. Park, T.H.T. Nguyen, E. Jin, Improving lipid production by strain development in microalgae: Strategies, challenges and perspectives, Bioresour. Technol. 292 (2019) 121953, https://doi.org/10.1016/j.biortech.2019.121953.